

NASA TECHNICAL MEMORANDUM

NASA TM-75711

THE SIGNIFICANCE OF WING END CONFIGURATION  
IN AIRFOIL DESIGN FOR CIVIL AVIATION AIRCRAFT

H. Zimmer

Translation of "Die Bedeutung der Fluegelendformen  
beim Tragfluegelentwurf fuer flugzeuge der zivilen  
Luftfahrt", Deutsche Gesellschaft fuer Luft- und  
Raumfahrt, Jahrestagung, 10th, Berlin, West Germany,  
Paper 77-030, Sept. 13-15, 1977, 40 pages

(NASA-TM-75711) THE SIGNIFICANCE OF WING  
END CONFIGURATION IN AIRFOIL DESIGN FOR  
CIVIL AVIATION AIRCRAFT (National  
Aeronautics and Space Administration) 35 p  
HC A03/MF A01

N80-10104

CSCS 01A G3/02

Unclas  
39367

REPRODUCED BY  
NATIONAL TECHNICAL  
INFORMATION SERVICE  
U.S. DEPARTMENT OF COMMERCE  
SPRINGFIELD, VA. 22161

NATIONAL AERONAUTICS AND SPACE ADMINISTRATION  
WASHINGTON, D.C. 20546  
OCTOBER 1979

## NOTICE

THIS DOCUMENT HAS BEEN REPRODUCED FROM THE BEST COPY FURNISHED US BY THE SPONSORING AGENCY. ALTHOUGH IT IS RECOGNIZED THAT CERTAIN PORTIONS ARE ILLEGIBLE, IT IS BEING RELEASED IN THE INTEREST OF MAKING AVAILABLE AS MUCH INFORMATION AS POSSIBLE.

1. Report No. NASA TM-75711		2. Government Accession No.		3. Recipient's Catalog No.	
4. Title and Subtitle THE SIGNIFICANCE OF WING END CONFIGURATION IN AIRFOIL DESIGN FOR CIVIL AVIATION AIRCRAFT				5. Report Date October 1979	
				6. Performing Organization Code	
7. Author(s) H. Zimmer, Dornier GmbH, Friedrichshafen, West Germany				8. Performing Organization Report No.	
				10. Work Unit No.	
9. Performing Organization Name and Address Leo Kanner Associates, Redwood City, California 94063				11. Contract or Grant No. NASw-3199	
				13. Type of Report and Period Covered Translation	
12. Sponsoring Agency Name and Address National Aeronautics and Space Administration, Washington, D.C. 20546				14. Sponsoring Agency Code	
15. Supplementary Notes Translation of "Die Bedeutung der Fluegelendformen beim Tragfluegelentwurf fuer Flugzeuge der zivilen Luftfahrt", Deutsche Gesellschaft fuer Luft- und Raumfahrt, Jahrestagung, 10th, Berlin, West Germany, Paper 77-030, Sept. 13-15, 1977, 40 Pages					
16. Abstract Lift-dependent induced drag in commercial aviation aircraft is discussed, with emphasis on the necessary compromises between wing end configuration modifications which better lift performance and the weight gains accompanying such modifications. Triangular, rectangular and elliptical configurations for wing ends are considered; attention is also given to airfoil designs incorporating winglets. Water tunnel tests of several configurations are reported. In addition applications of wing end modifications to advanced technology commercial aviation aircraft and the Airbus A-300 are mentioned.					
17. Key Words (Selected by Author(s))				18. Distribution Statement Unclassified-Unlimited	
19. Security Classif. (of this report) Unclassified		20. Security Classif. (of this page) Unclassified		21. No. of Pages 35	22. Price

## List of Symbols

A	Lift
b	Span
b'	Span of equivalent planar airfoil
$C_A, C_a$	Coefficient of lift
$C_{M-B}$	Coefficient of root bending moment (Fig. 10)
$C_S$	Coefficient of thrust
$C_{W_i}$	Coefficient of induced drag
$C_W$	Coefficient of drag
F	Airfoil surface, airfoil reference surface
G	Airfoil weight
h	Height of airfoil system
LFC	Laminar Flow Control
$M_B$	Bending Moment at airfoil root
q	Dynamic pressure
Re	Reynold number
TNT	Airfoil of present technology
$U_\infty, V$	Upstream velocity
W	Drag
$W_{i_{ell}}$	Induced drag of planar elliptical airfoil
$W_i$	Induced drag
X, Y, Z,	Right-angled coordinate systems
$\alpha$	Angle of inclination
$\gamma$	Local circulation
$\epsilon_H$	Adjustment angle of elevator unit
$\eta$	Dimensionless span

List of Symbols (continued)

$\eta_k$	Angle of deflection of flap
$\vartheta$	Winglet angle of inclination
$x$	Induced drag related to value of planar elliptical airfoil of the same extension
$\lambda$	Extension
$\rho$	Air density

THE SIGNIFICANCE OF WING END CONFIGURATION  
IN AIRFOIL DESIGN FOR CIVIL AVIATION AIRCRAFT

H. Zimmer  
Dornier GmbH, Friedrichshafen, West Germany

1. Introduction

In general aviation two problem areas have gained attention /2\* in the past years, the solution of which is aimed for via a critical review of the classical airfoil theory:

- 1) Because air traffic is becoming more dense and above all because of the introduction of the large capacity aircraft, the structure of wake vortex had to be more closely examined [3], [16], [20], as it may become dangerous for a smaller aircraft following if caught in the wake of a large capacity airplane;
- 2) climbing fuel costs force development of more economical aircraft than presently exist [5], [21].

Each problem area is interwoven with the other, as suitable airfoil modifications are the only means of dealing with them.

The present report is concerned with the second problem of drag reduction. Here, too, there are several areas from which to make a beginning. A large portion of aircraft drag is due to surface friction. Studies are being conducted on decreasing this portion by means of artificial laminarization or also via a yielding wall [21]. Other measures consist in decreasing trim drag through active control. Interference drag, caused by the interaction of aircraft and drive parts may also be reduced with the aid of suitable design [5]. Another significant portion is /3

---

\* Numbers in the margin indicate pagination in the foreign text.

profile drag. Application of the principles of supercritical aerodynamics led to improvements in high and low velocity ranges at Dornier [22], [23].

Subject of the following study is the lift dependent induced drag.

Aircraft performance in commercial aviation (e.g. climb rate and range) may only be improved - given the above-mentioned contributors to drag - by designing airfoils of greater span, or length, than have been normally applied to the present time. In the case of a square airfoil, for example, induced drag may be reduced by approx. 11 % by increasing extension from 8 to 9 in climbing, but a problem lies in the fact that airfoil weight increases by approx. 12 %. In order not to endanger the increase in aerodynamic performance by the increased structure weight, extensive studies were carried out recently, some of which will be briefly reviewed here.

## 2. Basic Data

The greatest circulation gradient of an airfoil naturally occurs at the outer ends. As a result of the flow around the wing tips and the boundary turbulence the airfoil flow also exhibits greatest deviation from the two-dimensional profile flow. This shows that special attention must be paid to the wing ends in wing design.

4

Basic knowledge on induced drag stems from the beginnings of the airfoil theory. As an example in Fig. 1 the induced drag of several non-planar configurations is compared with that of the elliptical airfoil [1], [2], [4], [5]. Non-planar configurations are therefore suitable for obtaining a considerable reduction in induced drag at a given span. This figure also shows, for example, that wing tips with several slots and end plates have approximately the same effect. Since a significant decrease in induced drag is possible using these, they have again become the

subject of numerous studies in the past years.

In the case of an aircraft, however, interest is not so much centered on this relationship of induced drag to that of elliptical airfoil as the induced drag itself. Through the simple considerations in Fig. 2 below it becomes clear that in the expression for induced drag the influence of span dominates, as this occurs as a square function, while the ratio of induced drag is only linear. In this figure various non-planar airfoil systems with a very low relative induced drag are compared with the planar single airfoils of identical actual induced drag, having in each case a corresponding calculated larger span. In examples 3 to 5 the single airfoil would have a span 41 % larger, as indicated, but it cannot be simply stated which airfoil system could be constructed with less cost and weight. In addition, present aspects of construction forbid such relatively high airfoil systems, leading to a substantially smaller difference in practical wing design. /5

### 3. Other Studies

At this point a brief review of other studies in this area with respect to the practical applications is of interest. Example 6 following Fig. 2 with a 15 % winglet height corresponds to a spanloader project of Boeing [6], shown in Fig. 3 with other configurations, also with three winglets. The high glide number of the configuration in [5], however, could only be achieved with the aid of artificial laminarization (Fig. 3, middle). The configuration in [7] (below) was tested in flight. Low drag and decreased wake vortex intensity was proven. Note the opposite stagger of winglet of the upper two configurations in comparison to that below. Two further spanloader configurations with large endplates are shown in Fig. 4 as in [8] and [9]. In Fig. 5 the Whitcomb winglets are shown as in [5], [10], [11], [18], [19]. (The project described in [18] has since been cancelled). Their winglets in a form ready for application, modified for a short takeoff and landing aircraft (IAI-Arava in [12], [24]), can be seen in Fig. 6 above. In this figure another two wing end forms often employed in general aviation are shown [13].



In an experimental and theoretical study various wing end forms were also examined at Dornier with the aim of achieving a drag reduction while maintaining smallest possible structural and weight disadvantages, respectively, expressed in wetted surfaces and airfoil root-bending moment.

#### 4.1 Experiment

The most interesting results from the first measuring phase in the Dornier water tunnel [15] are summarized in Fig. 7 in the form of polar curves of drag. Various wing end forms were attached to a rectangular half span model [17]. As can be seen in the polar curves, the configurations 2 and 3 with triangular edge and four winglets, respectively, are distinctly better than the rectangular wing except for a small drawback in zero drag. This is, of course, not surprising, since comparable forms causing vortex fanning out are employed almost without exception in nature. It was further demonstrated that interference of winglets to one another is very important. When two each are positioned as in configuration 3 in the optimum biplane arrangement in [25], [26], [27], the polar curve is favorable; however, when evenly arranged as in configuration 4, the polar curve is considerably more unfavorable, although there should be hardly any difference according to calculations. A series of other wing end forms were studied (Fig. 8). These are, however, uninteresting for application because of the greater detrimental drag.

#### 4.2 Theory

It was concluded in the analysis of measurement results and the flow observations that along with the simple triangular edge a slotted airfoil edge with triangular shape should also be of interest (Fig. 9). The two winglets are again positioned in this figure in the most favorable biplane arrangement possible. Other angle positions, however, were also studied.

Calculations were carried out with the aid of the vortex-end procedure in [14]. As indicated in Fig. 10, the influence of various wake forms was examined. Since wings of average extension are generally employed in aviation (6 - 12), calculations were not based on a self-adjusting wake vortex, but rather a fixed choice was made of these various forms and they were then compared with one another.

The differences in theoretical induced drag amount to approx. 1 % with a lift coefficient of 1.2. The difference does not increase until in the case of form 5, as a result of dissipation, a wake vortex shorter than 20 airfoil depths is assumed. For reasons of simplification the non-linear wake form 2 was therefore used as a base in all subsequent calculations.

For airfoil weight the following relation was used as a first approximation, i.e. the change of wetted surface and the change of airfoil root-bending moment are a direct measure of change in airfoil weight.

As an example from the calculations the local coefficients of lift and induced drag of the slotted and the triangular wing edge in Fig. 9 are compared to one another in Fig. 11. By means of the slotted form the tips on the outer edge are reduced. It is further noteworthy that winglet A generates a thrust as a result of its forward positioning as shown in Fig. 9. /8

#### 4.2.1 Airfoil Comparison at the Same Extension

A theoretical comparison was made now between planar and non-planar wing end forms. As can be seen in Fig. 12 the comparison was first carried out at the same extension. Here lift, wing root-bending moment and induced drag of the rectangular airfoil and two airfoils with variously pointed triangular edge were compared with the values of the elliptical airfoil. It was demonstrated that the airfoil with backwards pointing triangular edge behaves as an elliptical airfoil with the exception of small differences, whereas the

airfoil with forward pointing triangular edge behaves as a rectangular airfoil as far as drag is concerned. The rectangular airfoil has the largest relative weight.

The comparison of various airfoils is carried out with a lift coefficient of 1, approximately corresponding to climbing. This case is of special significance for flight safety in general aviation, as a reduction in drag by engine failure greatly affects the remaining climbing capability.

In Fig. 13 the data of the most important airfoils studied is summarized. First shown is the induced drag and then a simple formulation of friction drag influenced by the wetted surface, the two of which together compose the total drag. In column A the position numbers are listed only if the aerodynamic performance of each individual arrangement is taken into consideration. Thus the airfoil with the Whitcomb winglets is in position 1, the slotted airfoil edge in Fig. 9 in position 4 and 3, respectively, the elliptical airfoil and the simple triangular edge in position 7 and the configurations from the water tunnel measurements of Fig. 7 with four winglets occupy the last positions. If only relative airfoil weight is taken into consideration, the order according to column B is headed by the elliptical airfoil, then there follow the airfoils with slotted and triangular edge in positions 2 and 3. The configurations with vertical winglets and endplates now assume positions 9 and 10. If the aerodynamic performance and the relative weight are now evaluated equally, the order in column A - B results. The slotted forms of Fig. 9 are in positions 1 and 2, the elliptical airfoil in position 3. The triangular edge and the vertical winglets occupy position 4 and the endplates follow with number 6. /9

It becomes clear from these results that the aerodynamic advantages of the airfoil with endplates may only be utilized when the considerably enlarged root-bending moment is dealt with correspondingly. In the spanloader configurations of Figures 3 and 4 this is done by evenly distributing the disposable load over the entire span, thus effecting an airfoil stress reduction. In the case of the modified

IAI-Arava in Fig. 6, the prerequisites are favorable in that the airfoil is supported by struts and the larger root bending moment is intercepted along the strut. However problems may occur in yawing with the roll control as shown in flight test of Arava.[12].

#### 4.2.2 Airfoil Comparison with Identical Area and Identical Base Airfoil

/10

Especially the comparison of identical airfoil area and identical base airfoil is of practical interest, as it is conceivable that airfoil edge form be subsequently modified in advance project stages or even in completed aircraft. In Fig. 14 several results of airfoil end forms are summarized, interesting for applications, i.e. they appear to be realizable without too great an expense. The airfoil ends on a rectangular airfoil of 7.07 extension were varied, so that the project area remained unchanged. Using these considerations there result various individual extensions. If the aerodynamic performance in Column A is taken into consideration, however, then the form with the spread winglets assumes position 1, the form with triangular edge position 2 and that with vertically placed winglets position 3. The conventional edge curve (D0-28) is at position 6 and the rectangular airfoil at position 7. When considering only the relative weight the last is now in the first position, followed by the conventional edge curve and in third place the slotted edge curve. Vertical winglets and endplates are the final positions. When aerodynamics and structure weight are evaluated equally, the edge form with spread winglets is first, followed by the slotted and the triangular form in second place, the vertical winglets and the endplates follow the conventional forms at the end.

#### 5. Studies at the DFVLR

/11

In connection with these results basic experimental studies were conducted by the DFVLR on a conceptual model of an airfoil of present technology for general aviation. In two measuring phases a rectangular airfoil was equipped with various planar and non-planar airfoil ends of identical projection area. Extensive

measurements were taken of force, pressure distribution and wake, in addition to making flow visible [28], [29]. The most important results of the first measuring phase in connection with the present studies may be seen in Fig. 15. The airfoil with triangular edge exhibits a drag reduced by 13 % in the upper  $C_A$  range as compared to the rectangular airfoil. The measured difference corresponds exactly to that expected in the calculations. Reason for the maximum lift not being especially high is the thin symmetrical profile (Fig.9).

In a further study the triangular edge was tilted up and down at various angles up to vertical (endplate) while maintaining the same surface. No improvements could be achieved in polar curve, in agreement with theoretical considerations and other studies (e.g. [17]).

In the second measuring phase the airfoil edge as in Fig. 9 was measured with the winglets in two positions. The most important results are shown in Fig. 16. The slotted form 5 has the best polar curve of all measured configurations, at small  $C_A$  values the spread form is of the same value. When  $C_A = 0.3$  the airfoil drag is 13 % less than that of the rectangular airfoil and 8 % less than that of the airfoil with triangular edge. This means that the calculated /12 thrust effect of the winglets A in Fig. 11 was confirmed in the measurements. It was additionally demonstrated, that this form has no greater zero drag than the rectangular airfoil. As is further shown in Fig. 16, the polar curve of the spread form 6 becomes less favorable with increasing coefficient of lift, although it should be better according to calculations than the slotted form. The tendency from the water tunnel measurements in Fig. 7 are again confirmed here, i.e. when the winglets do not have an optimal influence on each other, they do not lead to the desired effect. This effect is to be explained by the interaction of potential flow and boundary layer [27]. When only the potential flow is taken into consideration, erroneous results are achieved, in the case where several winglets are under observation (e.g. the slotted form is in position 4 in Fig. 14 according to calculations, but

in position 1 according to measurements).

## 6. Application of Results

It was demonstrated that even relatively small alterations on wing tips have a distinct influence on the polar curve. In addition results showed that modifications in the airfoil plane such as the simple and the slotted triangular edge are, on the whole, more effective than non-planar modifications. Therefore the application possibility of results achieved on two typical commercial aviation aircraft is discussed in conclusion.

### 6.1 Improvement of Climbing Rate

/13

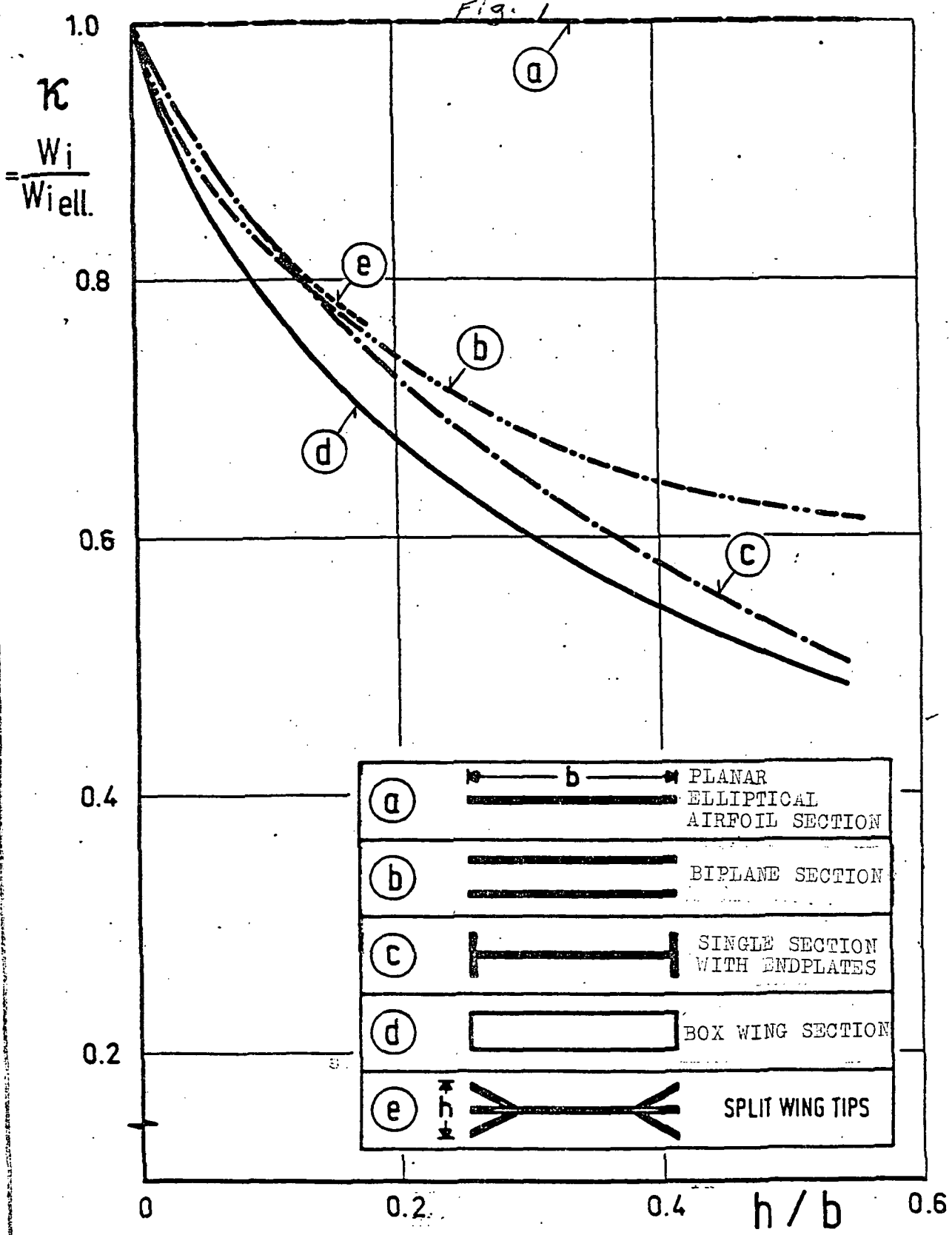
The airfoil of present technology developed at Dornier for general aviation was tested in a wind tunnel with various airfoil end forms. It was possible to be equipped with a conventional edge curve ("DO-28" type as in Fig. 15) and with a triangular edge. As the circulation distribution at the lower left shows for  $10^\circ$  angle of inclination, by means of the relatively small alteration the gradient of circulation becomes flatter over the entire span, meaning that the wake vortex intensity is reduced. The induced drag decreases in this case by approximately 10 %. Although the extension increases by 13 %, the relative airfoil weight increases by only 3.2 %. If an affine alteration of basic shape with conventional edge is made to achieve the same rise in extension, the weight increase would be four times as much with the same area. In Fig. 17 at the right the polar curve measured for the total arrangement as with both wing end forms is also given [30]. Although in normal flight ( $C_A \approx 0.3$ ) no difference occurs between polar curves, in climbing ( $C_A \approx 1.2$ ) a reduction of total drag of 10 % is determined.

### 6.2 Improvement in Range

In Fig. 18 several characteristic quantities of two subsonic transporters with modified wing ends are compared with one

another, specifically the Tanker KC-135 described in [11] with and without winglets and the Airbus A-300 with straight and triangular wing edge as described in [31]. The winglets, for example, reduce induced drag by 17 % and the total drag by 6.2 % while the triangular edge on the Airbus decreases the induced drag by 14 % and total drag by 5 %. Wing weight is increased here by 3.8 %, while when using these considerations the winglets increase the wing weight by 5.4 %. The decision has to be made whether to strengthen the wing subsequently and partially lose the gain in range once more, or to leave the main wing structure unchanged and limit maneuverability. /14

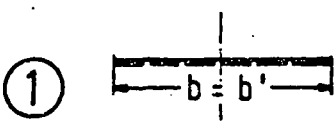
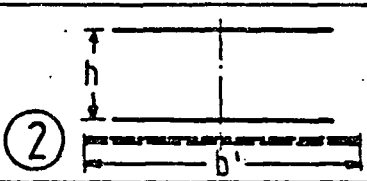
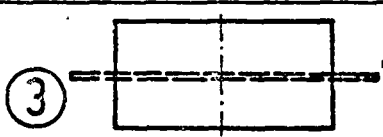
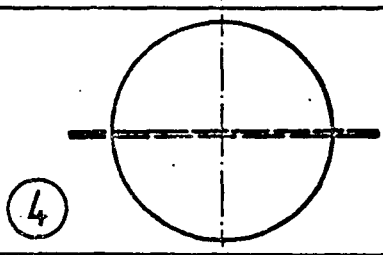
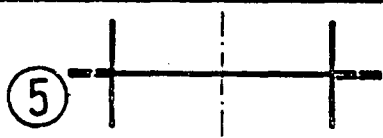
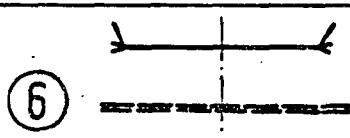
Fig. 1



RELATION OF INDUCED DRAG OF VARIOUS CONFIGURATIONS AT IDENTICAL LIFT AND IDENTICAL SPAN



Fig. 2

CONFIGURATION	IDENTICAL SPAN		IDENTICAL INDUCED DRAG	
	$h/b$	$\kappa$	$b'/b$	$\kappa'$
① 	0	1	1	1
② 	0.5	0.62	1.27	1
③ 	0.5	0.5	1.41	1
④ 	1.0	0.5	1.41	1
⑤ 	0.5	0.5	1.41	1
⑥ 	0.15	0.775	1.136	1

$$W_i = \kappa \cdot \frac{A^2}{\frac{g}{2} U_\infty^2 \pi b^2}$$

$$\frac{b'}{b} = \sqrt{\frac{\kappa'}{\kappa}}$$

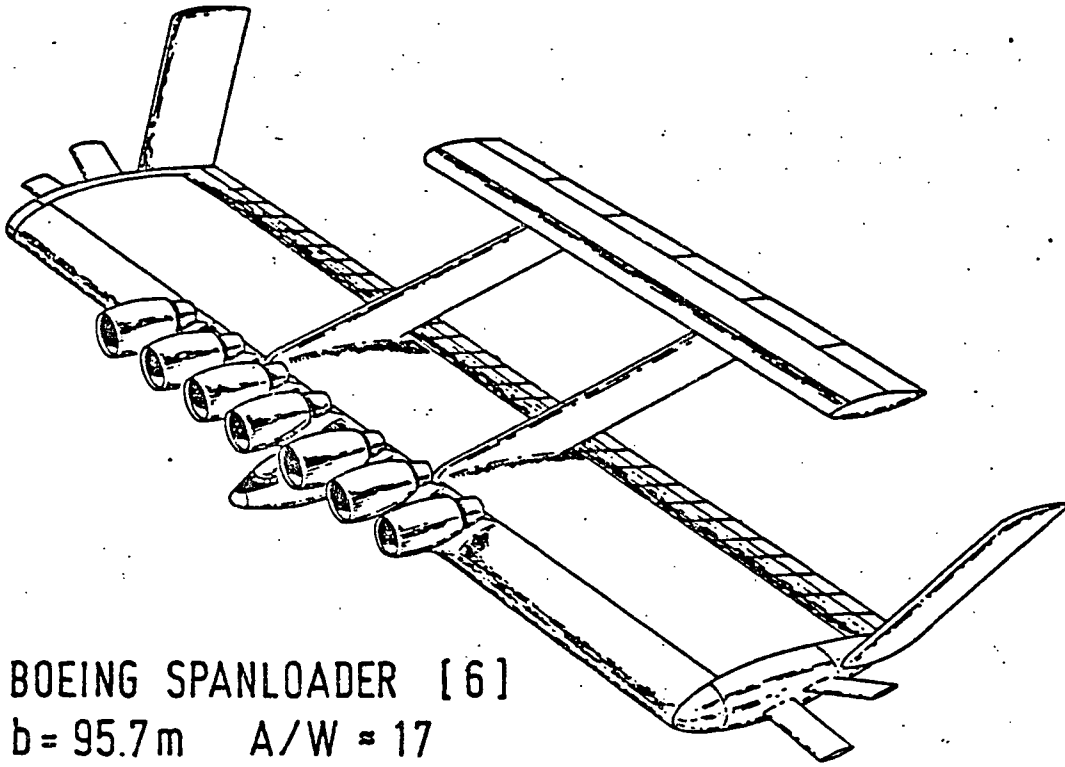
für:  
 $A = A'$   
 $W_i = W_i'$

ORIGINAL PAGE IS  
 OF POOR QUALITY

COMPARISON OF NON-PLANAR SYSTEMS  
 WITH THE SINGLE WING SECTION AT  
 IDENTICAL LIFT

72

Fig. 3



BOEING SPANLOADER [6]  
b = 95.7m A/W = 17

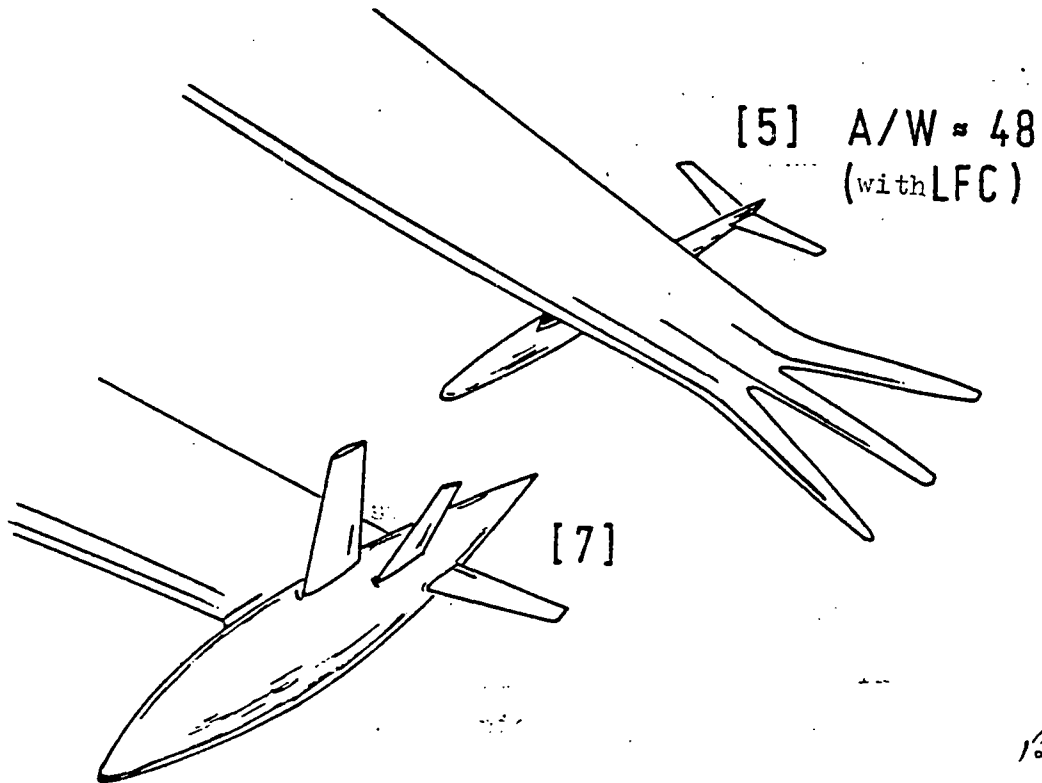
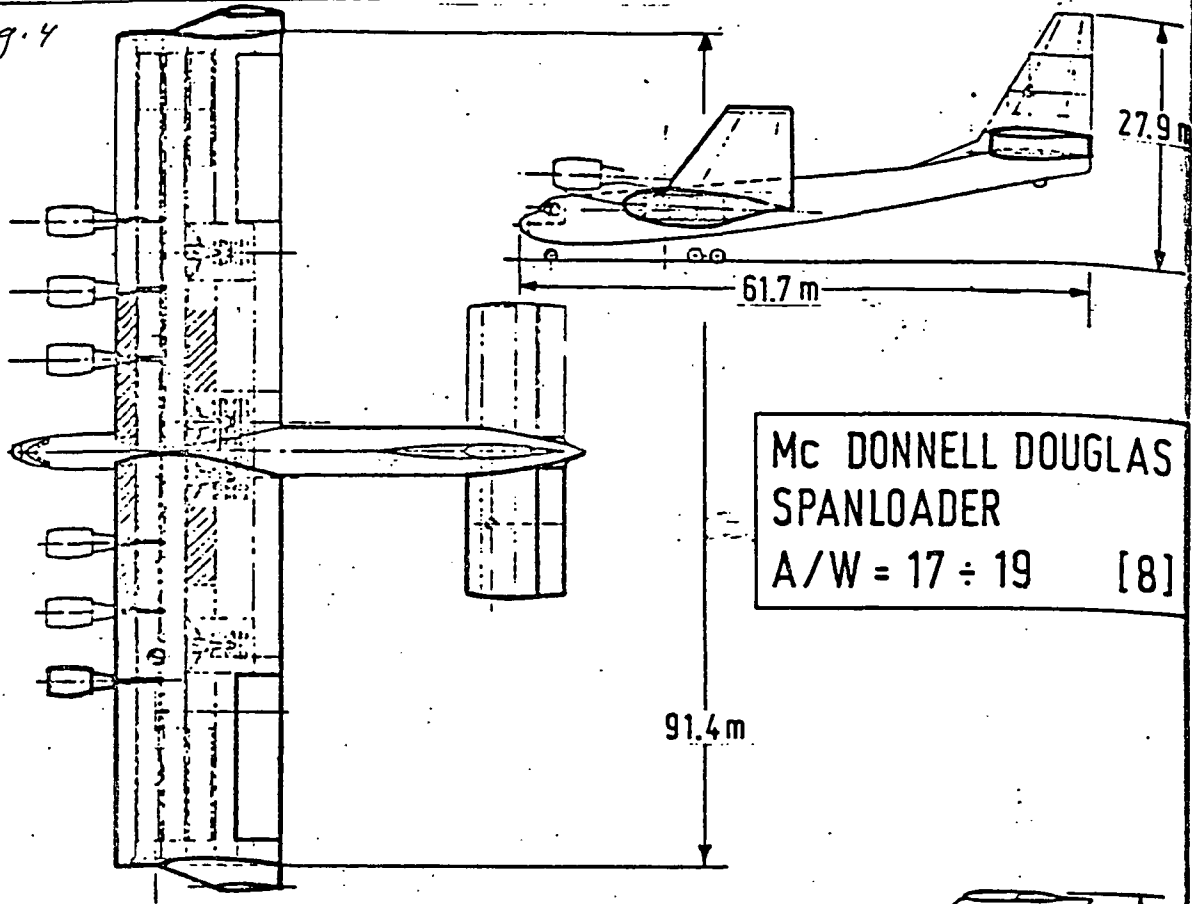


Fig. 4



ORIGINAL PAGE IS  
OF POOR QUALITY

LOCKHEED  
SPANLOADER  
A/W ≈ 20 [9]

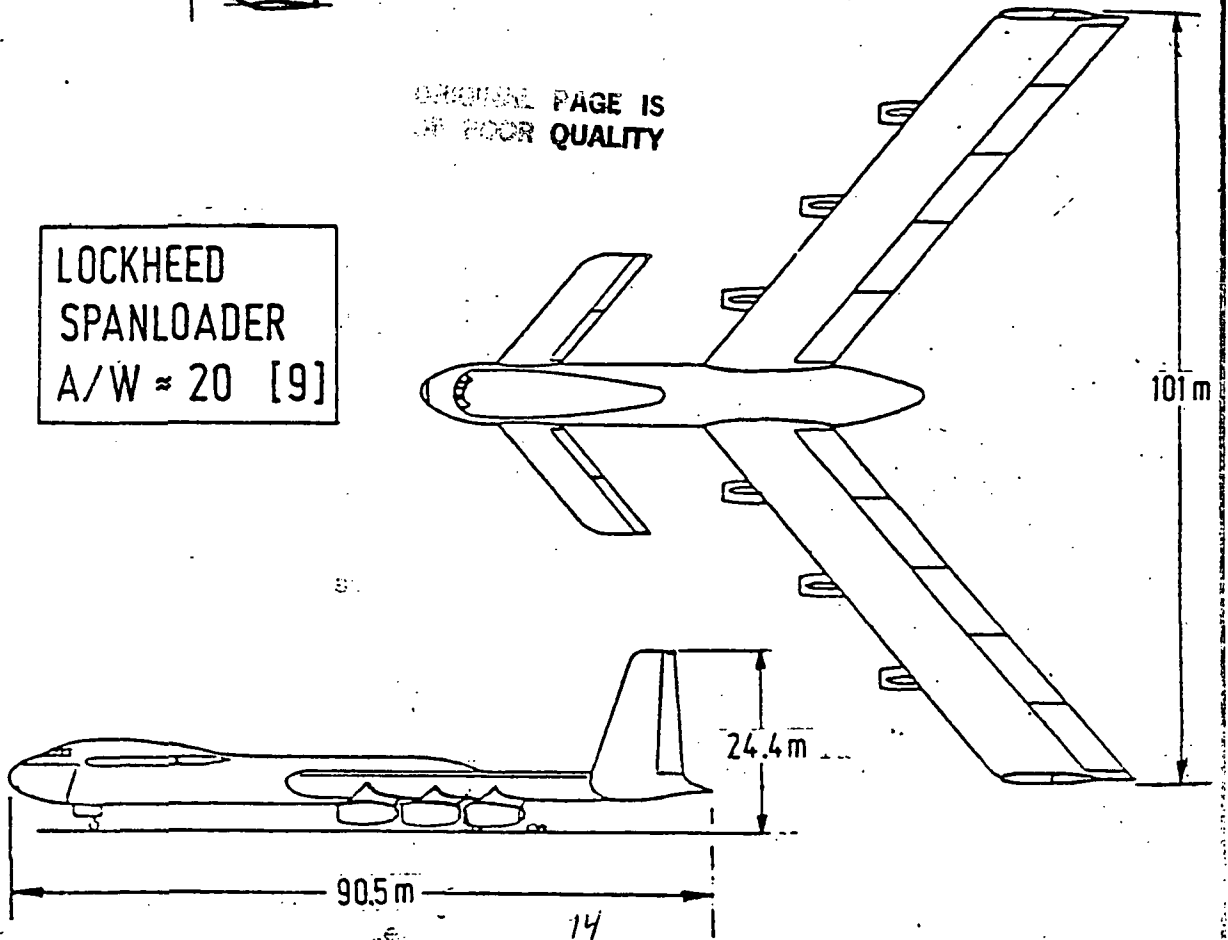
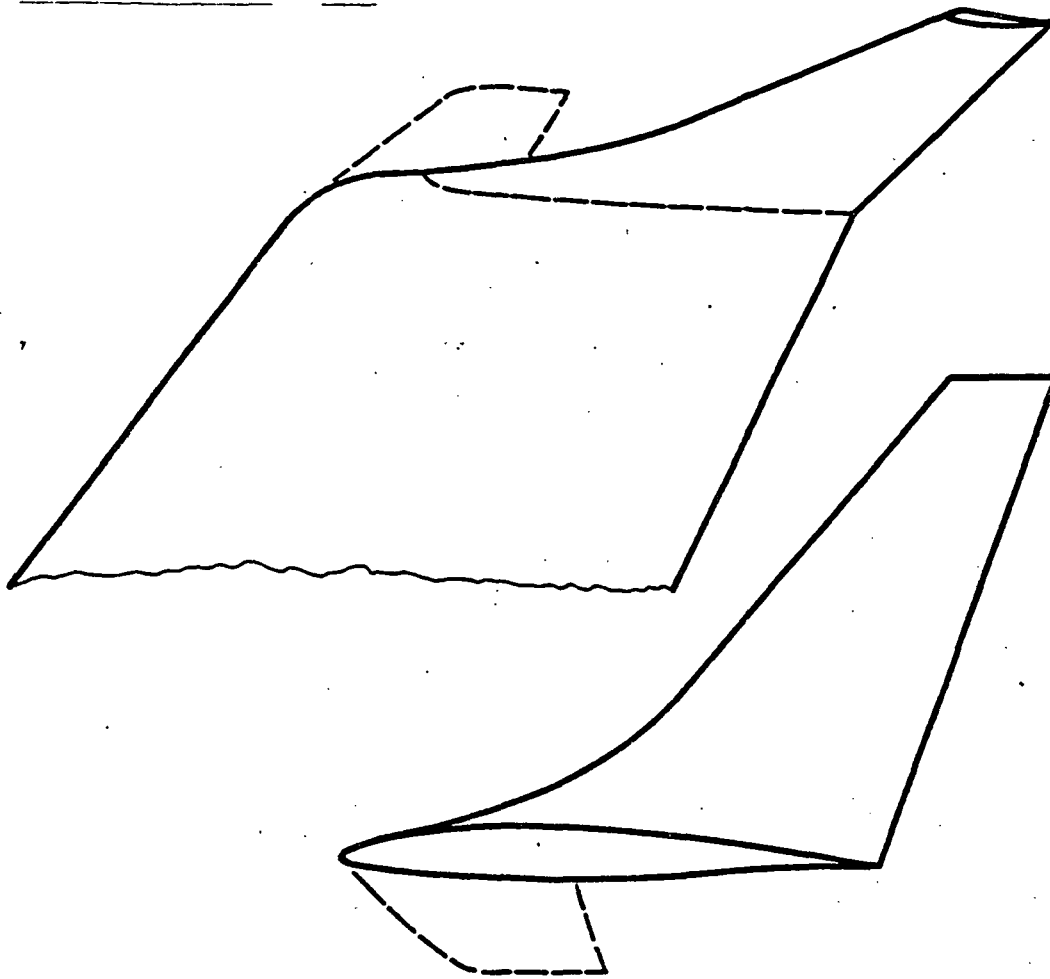
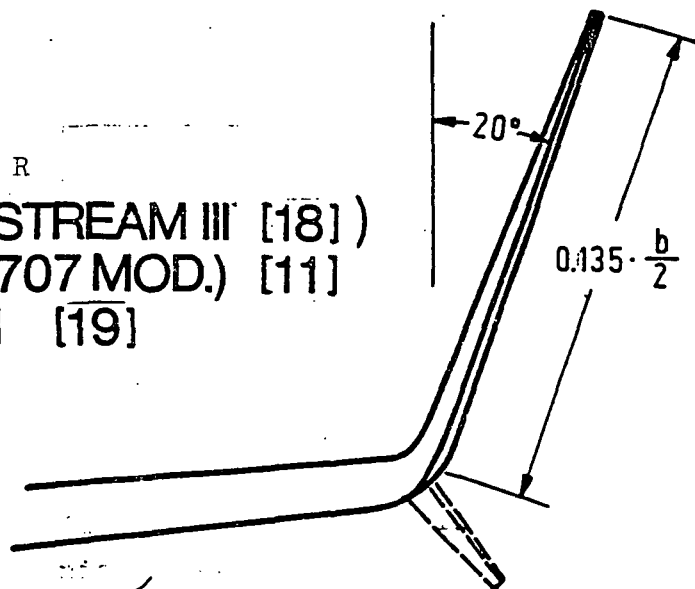


Fig. 5

WINGLETS [10]



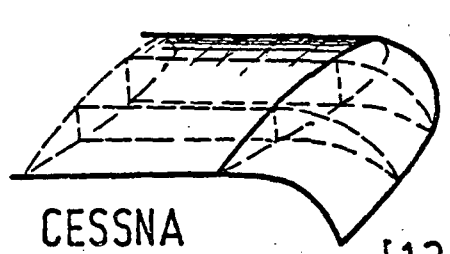
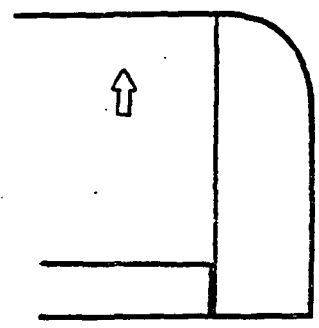
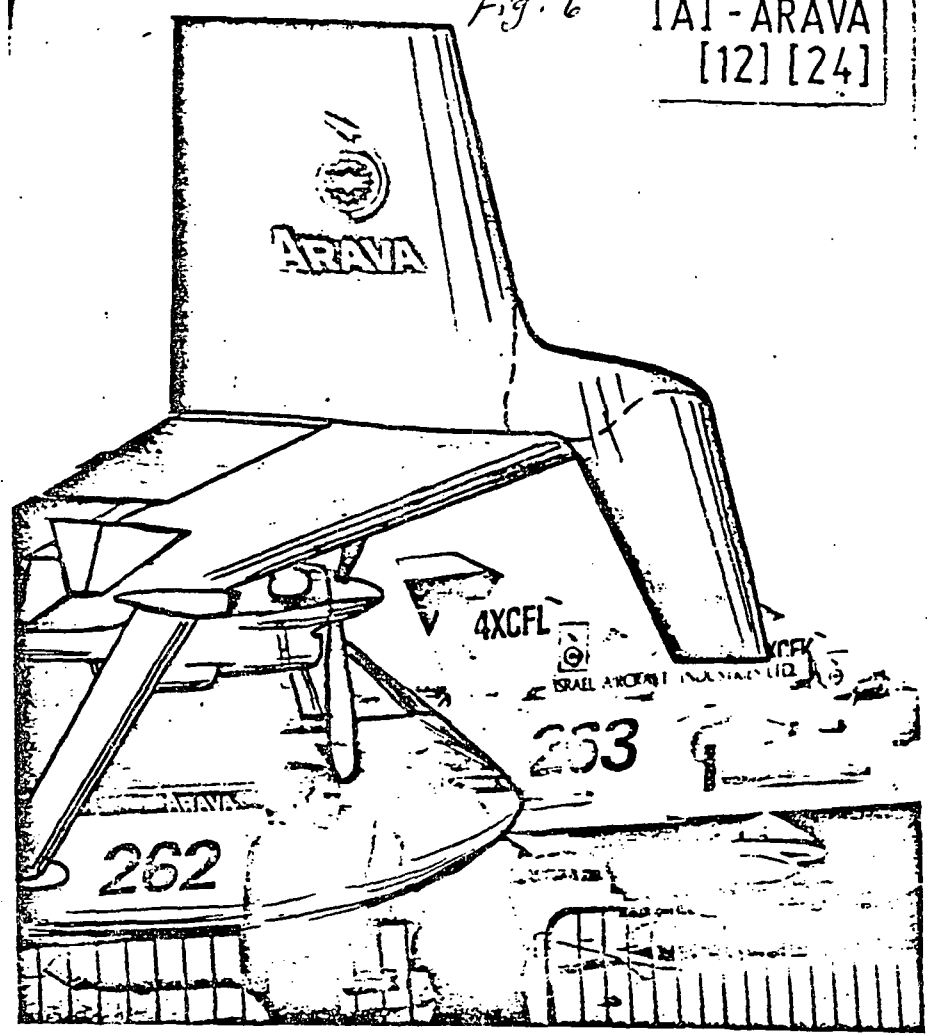
DESIGNED FOR  
(GRUMMAN GULFSTREAM III [18])  
BOEING KC-135 (707 MOD.) [11]  
LOCKHEED C-141 [19]



15

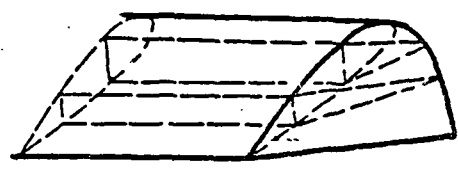
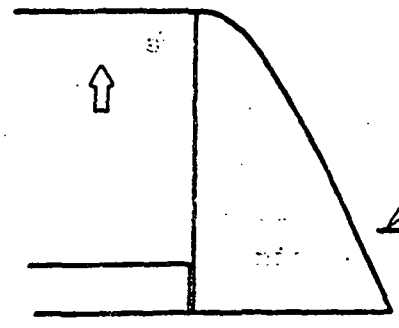
Fig. 6

IAI - ARAVA  
[12] [24]



CESSNA

[13]



BN TRISLANDER

16

WATER TUNNEL STUDY

a)

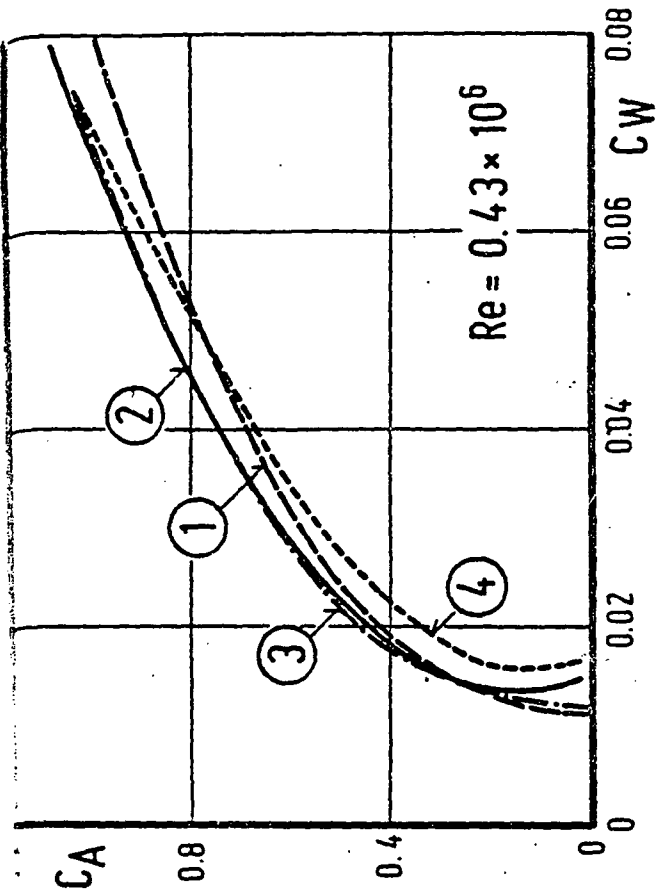
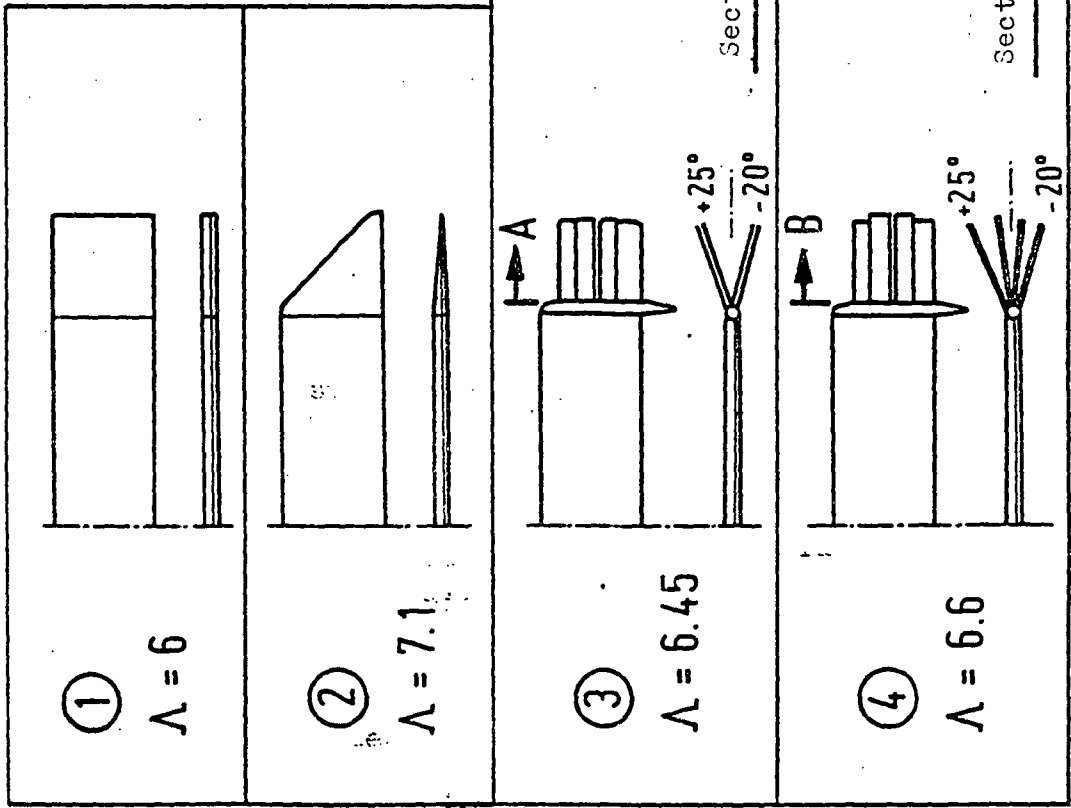


Fig. 1

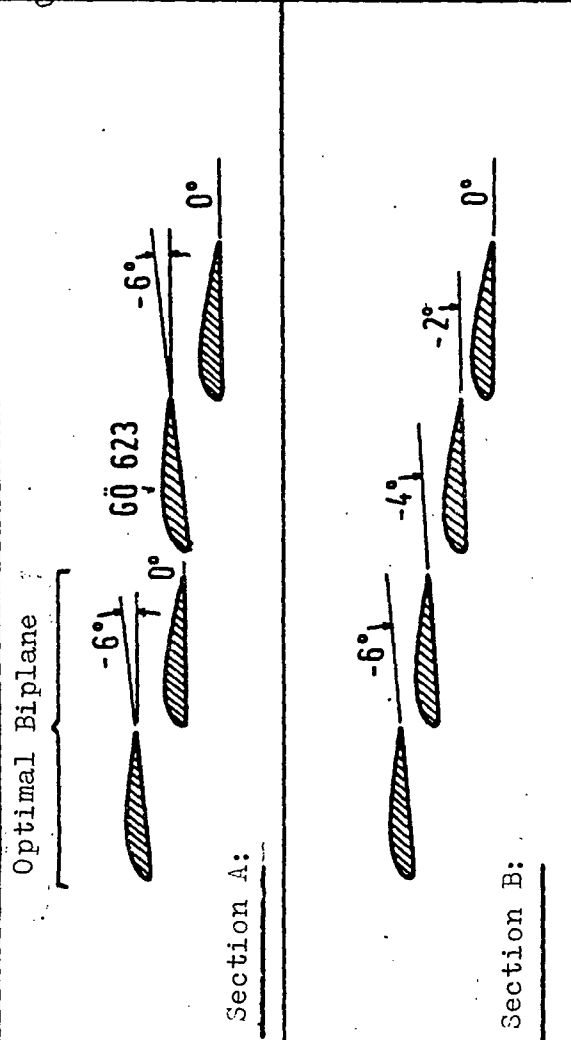


Fig. 8

WATER TUNNEL STUDY

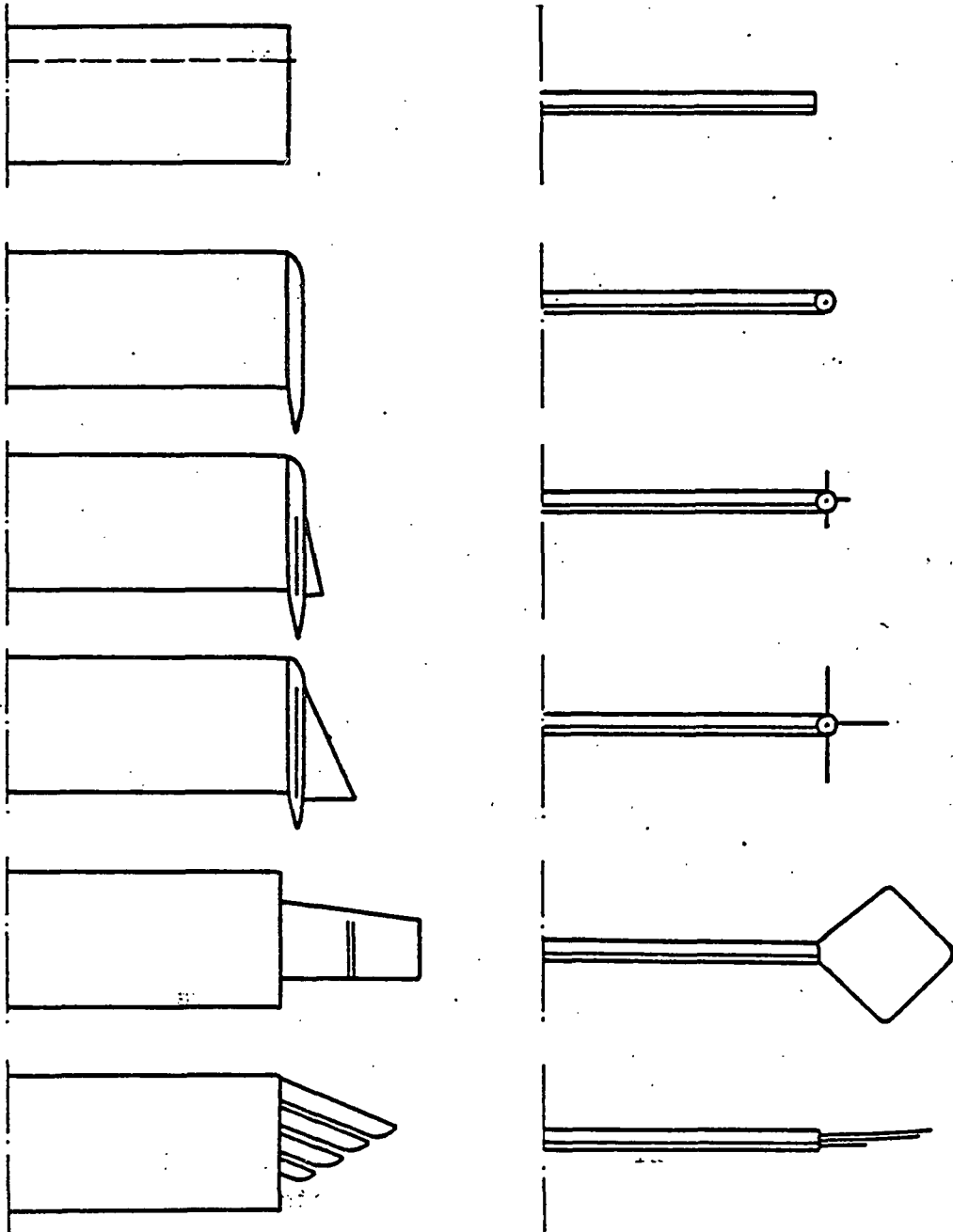
FURTHER AIRFOIL SHAPES

b)

Sc

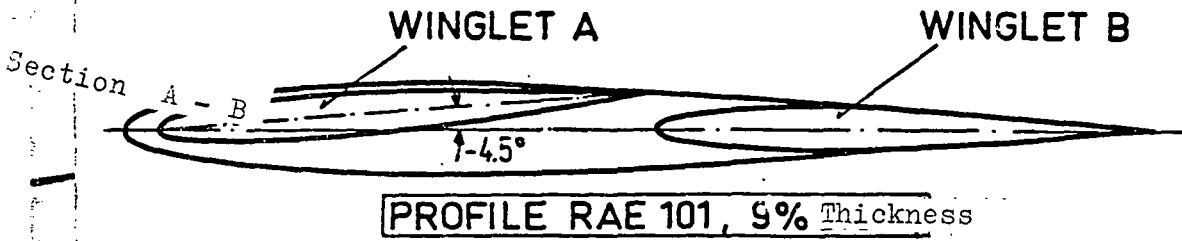
←

An



GE

Schnitt A - B



View from the Rear

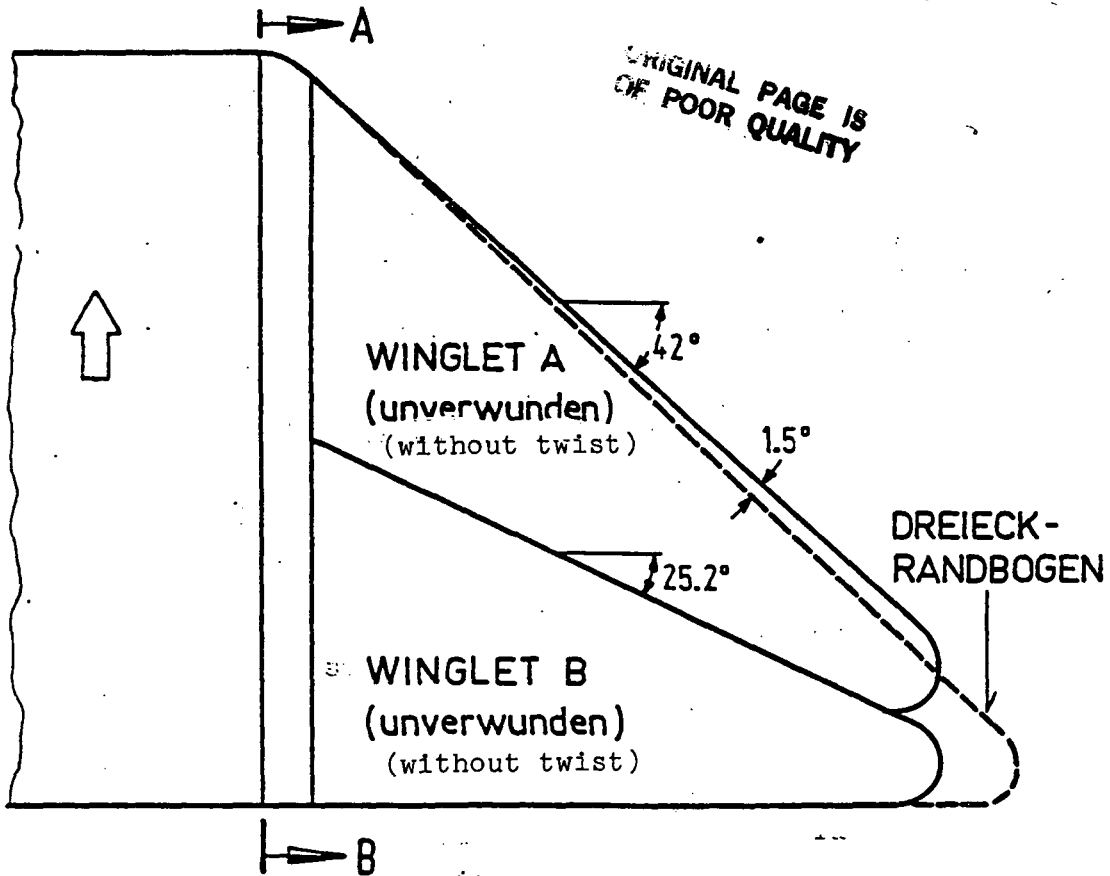
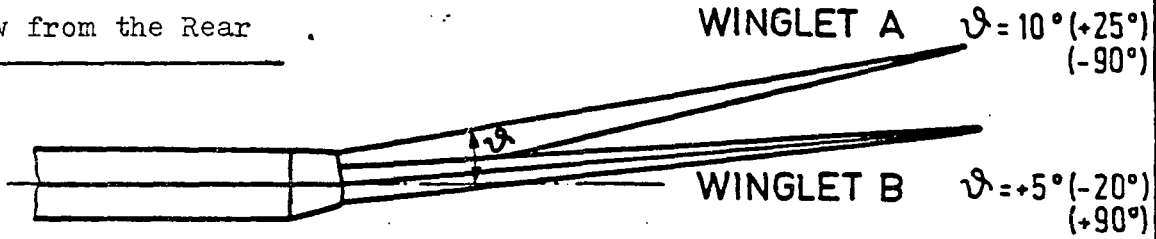




Fig. 10

Cutward Roll Tendency

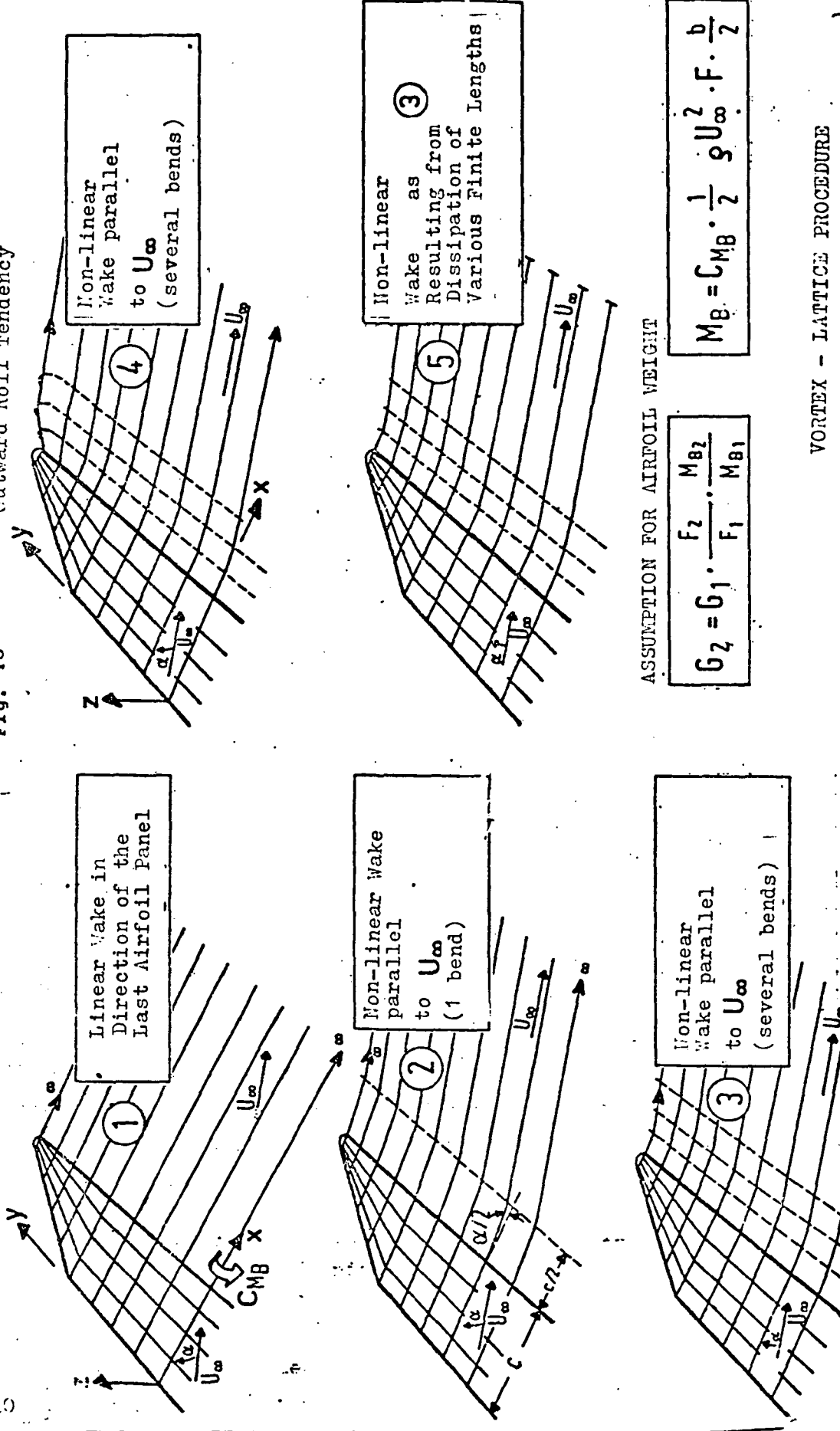
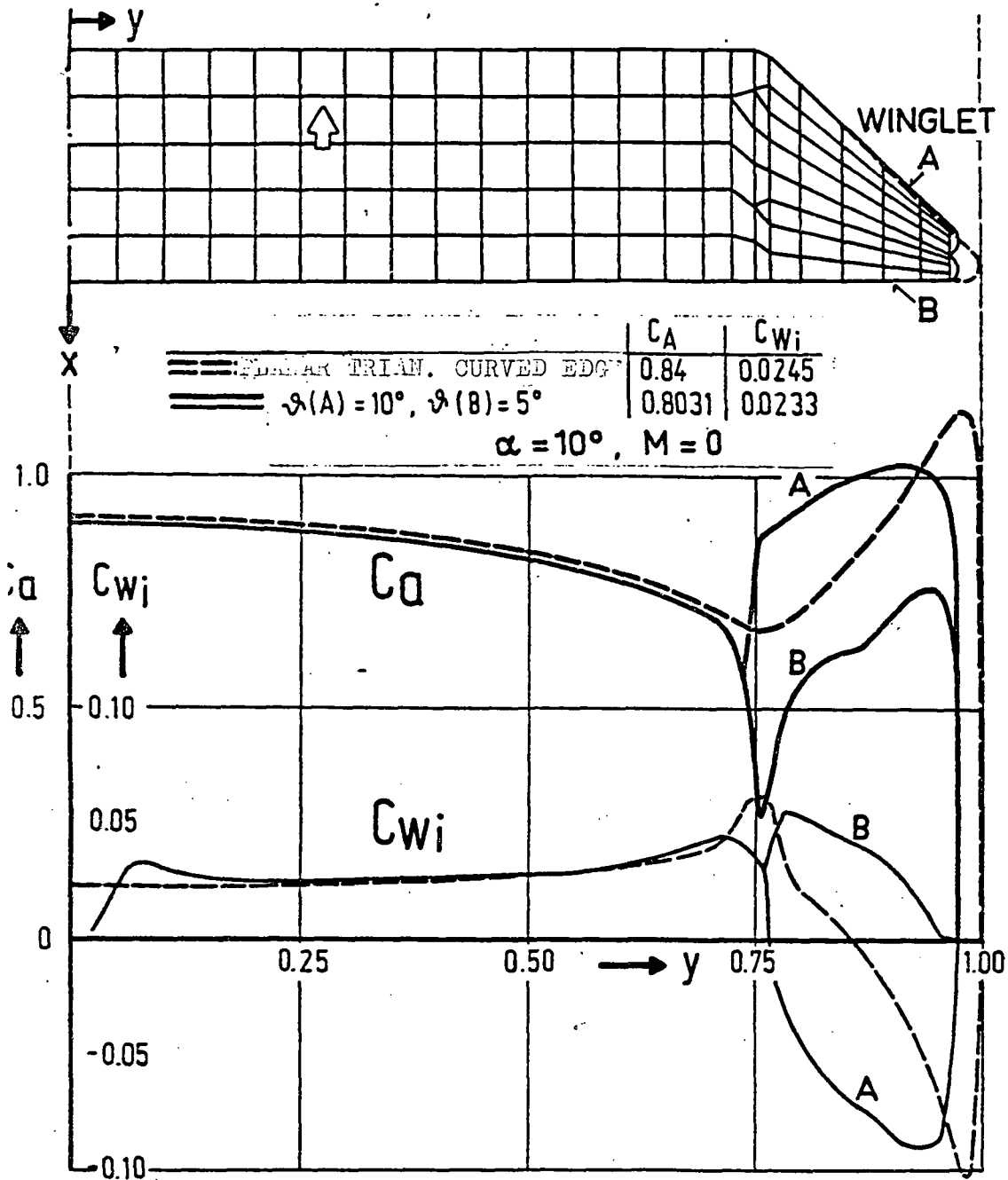
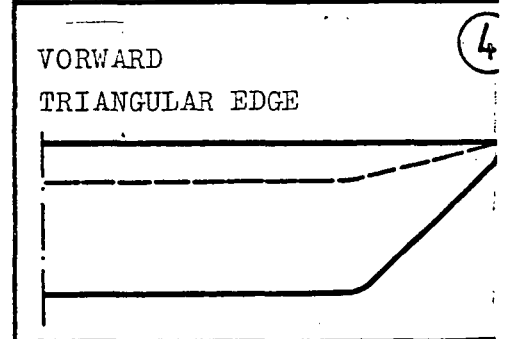
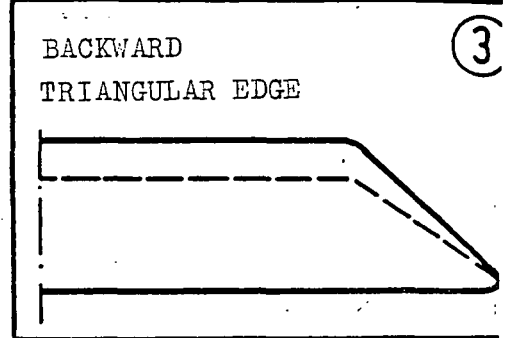
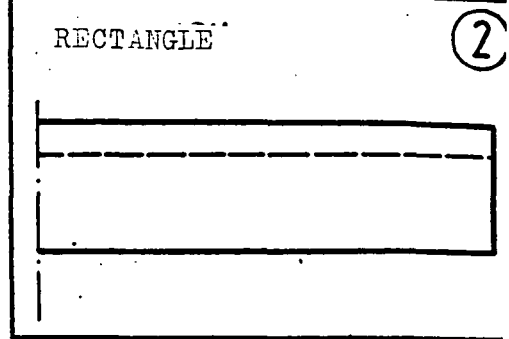
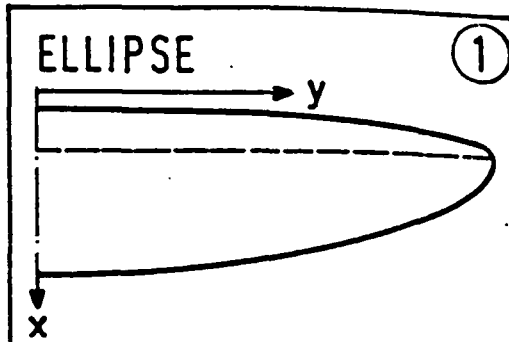
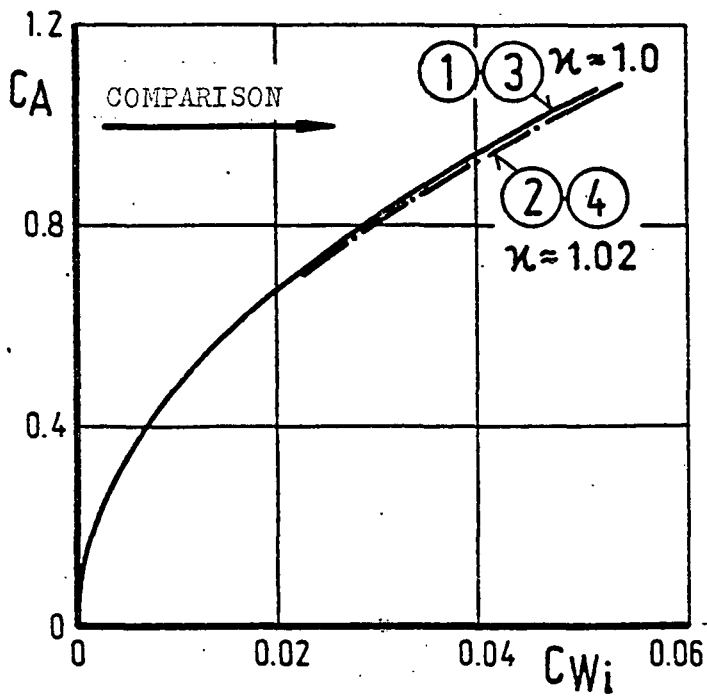
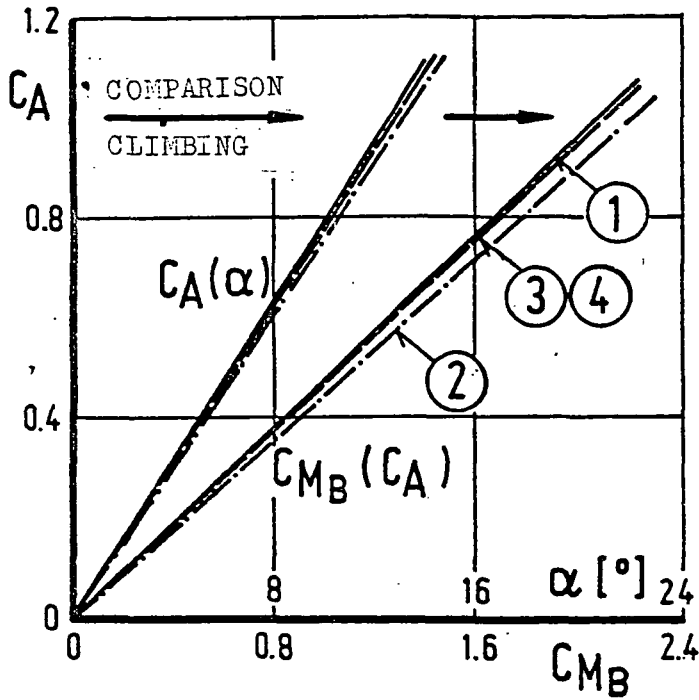


Fig. 11



LOCAL COEFFICIENT OF LIFT AND  
INDUCED DRAG

Fig. 12



COMPARISON OF VARIOUS AIRFOIL SHAPES AT THE SAME EXTENSION

$\Lambda = 7,05$  PLANAR

COMPARISON OF VARIOUS CONFIGURATIONS WITH EXTENSION 7.05 AT  $C_A = 10$


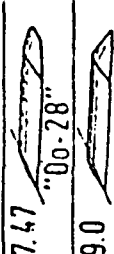
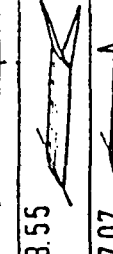



Fig. 13

Configuration	Induced Drag $C_{wi}$	$\frac{F}{F_{PLANAR}}$	Friction Drag $0.001 \cdot \frac{F}{F_{PLANAR}}$	Total Drag $C_w$	Place No. (A)	$\frac{C_{MB}}{C_{MBELL}}$	Relative Airfoil Weight $\frac{G}{G_{ELL}} = \frac{F}{F_{PLANAR}} \cdot \frac{C_{MB}}{C_{MBELL}}$	Place No. (B)	Place No. (A·B)
	0.045	1.0	0.02	0.065	7	1.0	1.0	1	3
	0.046	1.0	0.02	0.066	8	1.063	1.063	5	7
	0.045	1.0	0.02	0.065	7	1.02	1.02	3	4
	0.046	1.0	0.02	0.066	8	1.02	1.02	3	5
	0.046	1.006	0.02006	0.06606	9	1.226	1.232	7	8
	0.047	1.006	0.02006	0.06706	10	1.25	1.257	8	9
	0.039	1.369	0.02369	0.06269	5	1.039	1.421	11	8
	0.042	1.138	0.02138	0.06338	6	1.067	1.213	6	6
	0.0425	1.004	0.02004	0.06254	4	1.01	1.014	2	1
	0.0379	1.021	0.02021	0.05811	3	1.034	1.056	4	2
	0.0335	1.156	0.02156	0.05506	1	1.144	1.323	9	4
	0.0352	1.156	0.02156	0.05676	2	1.15	1.33	10	6

CA = 1

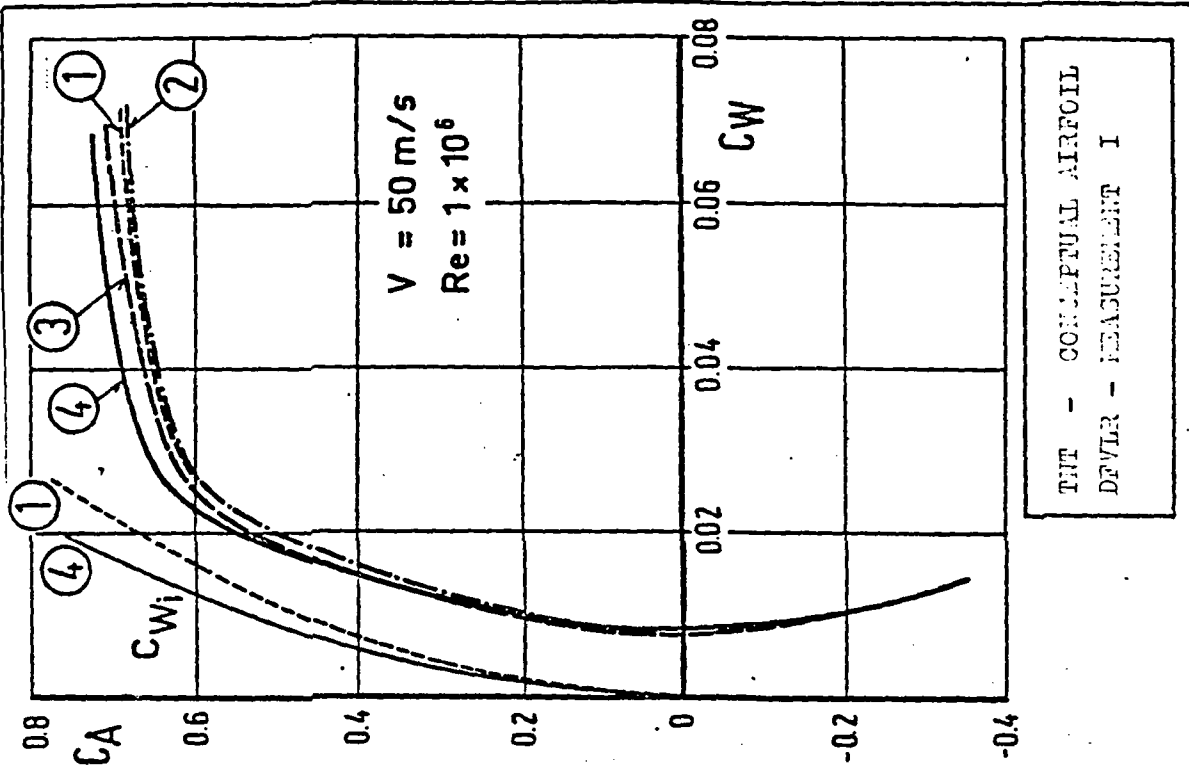
Comparison of various Configurations at identical area and identical airfoil section at

Fig. 14

Configuration	Induced Drag $C_{wi}$	$\frac{F}{F_{REC}}$	Friction Drag $0.01 \cdot 0.01 \cdot \frac{F}{F_{REC}}$	Total Drag	Place No. (A)	$\frac{M_B}{M_{B_{REC}}}$	Relative Airfoil Weight		Place No. (B)	Place No. (A-B)
							$\frac{G}{G_{REC}}$	$\frac{F}{F_{REC}} \cdot \frac{M_B}{M_{B_{REC}}}$		
 $\lambda = 7.07$	0.046	1.0	0.02	0.066	7	1	1.0		1	3
 7.47 "00-28"	0.043	1.0	0.02	0.063	6	1.031	1.031		2	3
 9.0 "TNT"	0.0347	1.0	0.02	0.0547	2	1.099	1.099		5	2
 8.56	0.0356	1.004	0.02004	0.05564	4	1.057	1.061		3	2
 8.55	0.033	1.01	0.0201	0.0531	1	1.066	1.077		4	1
 7.07	0.0335	1.156	0.02156	0.05506	3	1.0724	1.24		6	4
 7.07	0.0352	1.156	0.02156	0.05676	5	1.086	1.255		7	5

08 (1)

Fig. 15



CUT-OFF AIRFOIL END

$b = 2.1934 \text{ m}$   
 $\Lambda = 7.3113$

"GOTTINGER" CURVED EDGE

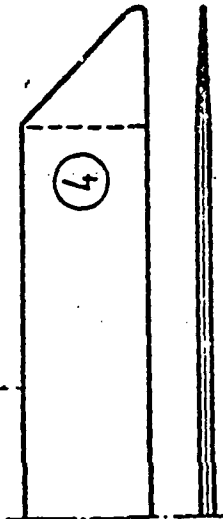
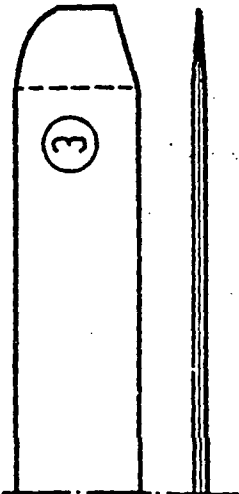
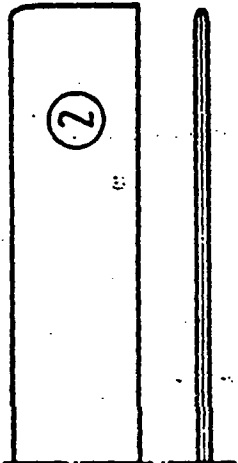
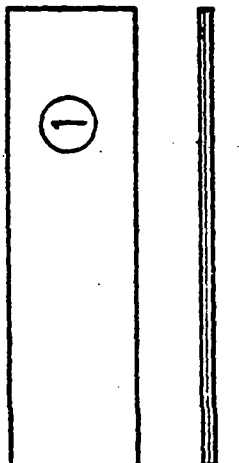
$b = 2.1954 \text{ m}$   
 $\Lambda = 7.3246$

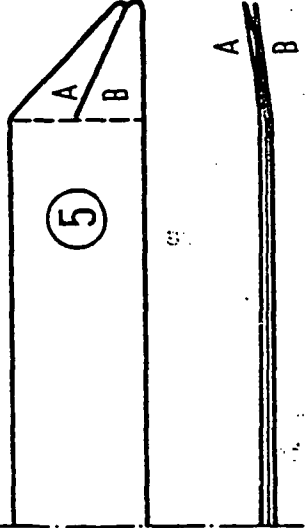
"DO 28" CURVED EDGE

$b = 2.2502 \text{ m}$   
 $\Lambda = 7.6949$

TRIANGULAR CURVED EDGE

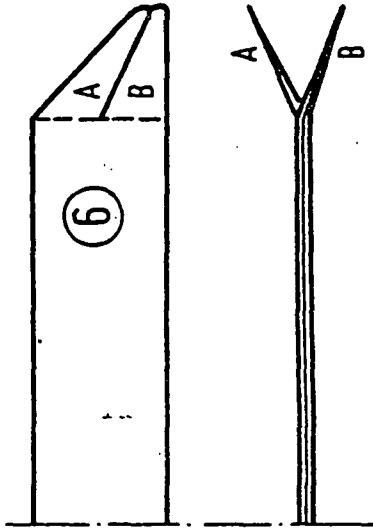
$b = 2.46 \text{ m}$   
 $\Lambda = 9.1967$





SLOTTED  
CURVED EDGE

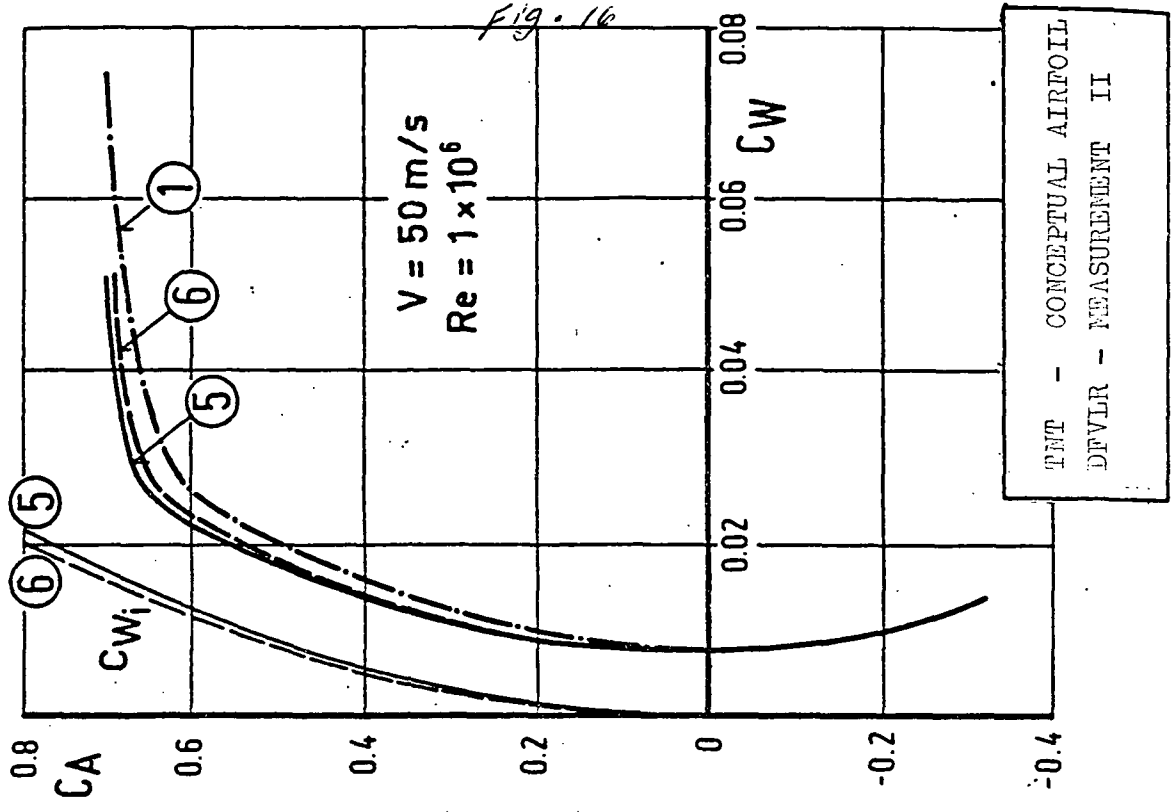
$\psi_A = +10^\circ$   
 $\psi_B = +5^\circ$   
 $b = 2.40 \text{ m}$   
 $\Lambda = 8.753$

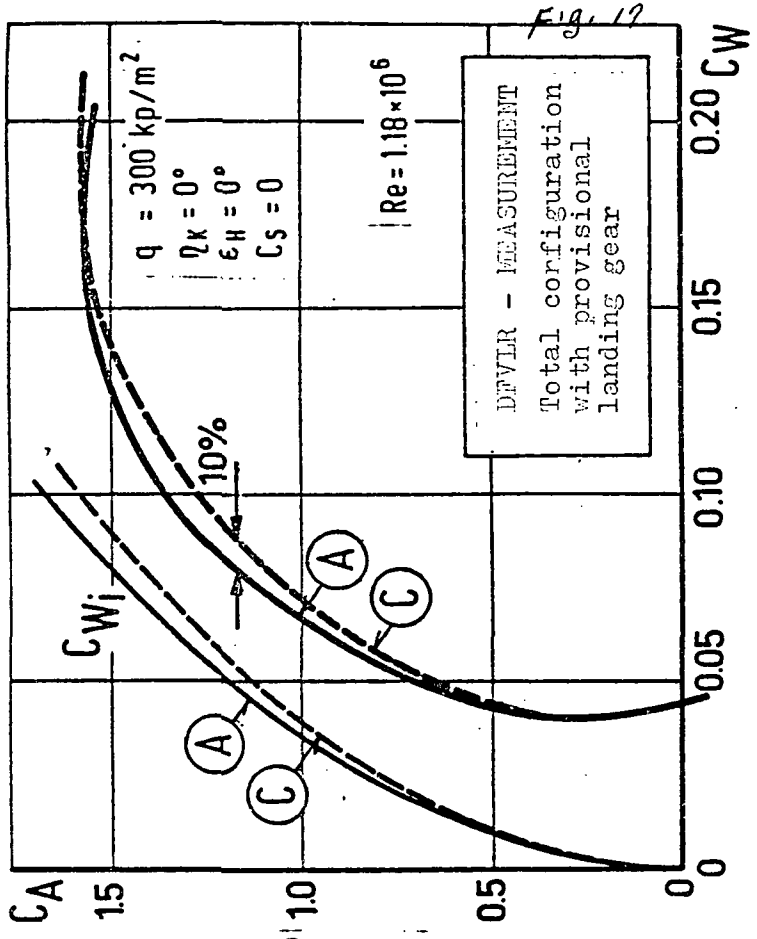
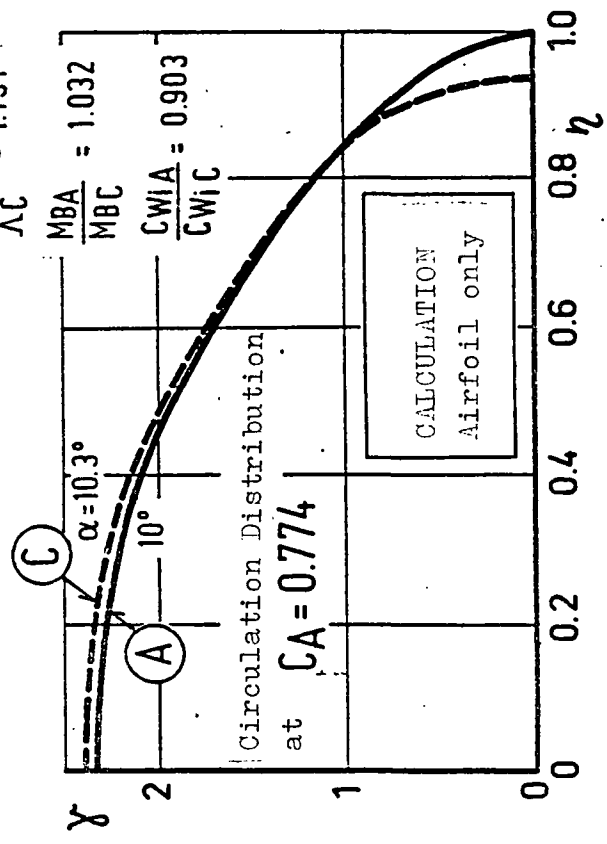
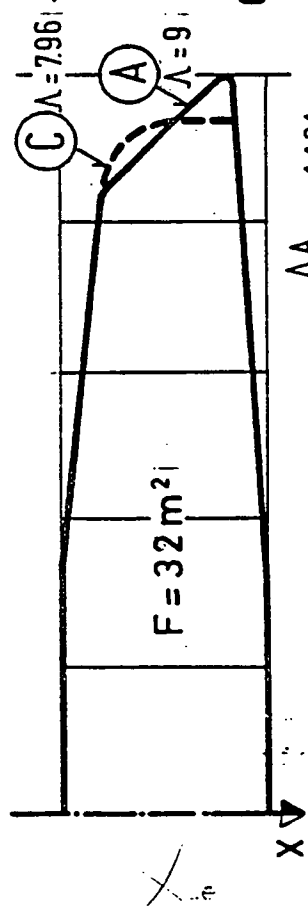
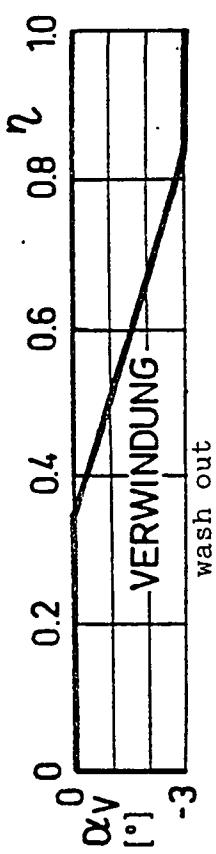


SPREAD  
WINGLETS

$\psi_A = +25^\circ$   
 $\psi_B = -20^\circ$   
 $b = 2.36 \text{ m}$   
 $\Lambda = 8.465$

Fig. 16



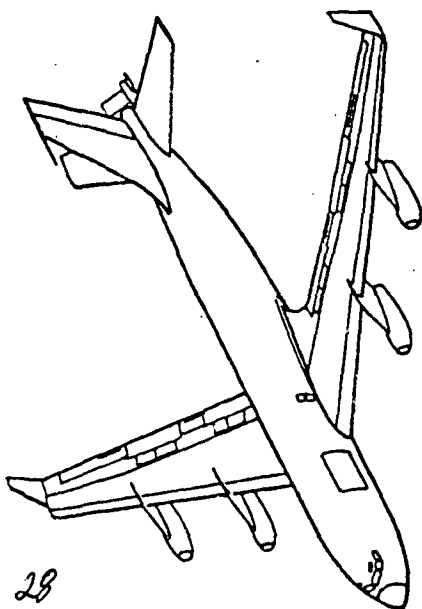


INFLUENCE OF THE AIRFOIL END FORM IN THE CASE OF "AIRFOIL OF PRESENT TECHNOLOGY"

Fig. 19



ORIGINAL PAGE IS  
POOR QUALITY



$\Lambda = 7.69$   
8.99

Fig. 18

PHYSICAL QUANTITY	KC-135			AIRBUS A-300		
	NORMAL-VERSION	WITH WINGLETS	CHANGE [%]	NORMAL-VERSION	MODIFIED AIRFOIL ENDS	CHANGE [%]
$\Lambda$	7.06	7.06	0°	7.69	8.99	+17
$b$ (m)	44.42	44.42	0	44.8	48.4	+ 8
$F$ (m <sup>2</sup> )	279	285.9	+ 2.2	260	260	0
$C_A$	0.45	0.45	0	0.486	0.486	0
$C_{wi}$	0.00875	0.00727	-17	0.00969	0.0083	-14
$C_w$	0.02642	0.0248	- 6.2	0.02769	0.0263	- 5
$A/W$	17	18.15	+ 6.8	17.57	18.5	+ 5.2%
$M_{B2}/M_{B1}$	1	1.031	+ 3.1	1	1.038	+ 3.8
$G_2/G_1$	1	1.054	+ 5.4	1	1.038	+ 3.8

COMPARISON OF KC-135 AND AIRBUS WITH MODIFIED AIRFOIL ENDS

## REFERENCES

- [1] Munk, M., Isoperimetrische Aufgaben aus der Theorie des Fluges (Isoperimetrical Calculations based on the Theory of Flight), Inaugural Dissertation, Göttingen, 1919.
- [2] Prandtl, L., Betz, A., Ergebnisse der Aerodynamischen Versuchsanstalt zu Göttingen (Results of the Aerodynamic Research Institute at Göttingen), Installments I - III, Berlin, 1923.
- [3] Hallock, J.N., "Aircraft Wake Vortices - An Annotated Bibliography (1923 - 1975)," Report No. FAA-RD-76-43, January 1976.
- [4] Cone, C.D., "The Theory of Induced Lift and Minimum Induced Drag of Nonplanar Lifting Systems," NASA TR R-139, 1962.
- [5] Whitcomb, R.T., Pfenniger, W., et al, "Special Course on Concepts for Drag Reduction," AGARD Report No. 654, March 1977.
- [6] Whitlow, D.H., Whitener, P.C. (Boeing), "Technical and Economic Assessment of Span-Distributed Loading Cargo Aircraft Concepts," NASA CR-144963, June 1976.
- [7] Wilkinson, K.G., "The Role of Technology in Air Transport - 2000 AD," Aircraft Engineering, 23 - 30 (May 1977).
- [8] McDonnell Douglas Corporation, "Technical and Economic Assessment of Span-Loaded Cargo Aircraft Concepts," NASA CR-144962, January 1976.
- [9] Lockheed Georgia Company, "Technical and Economic Assessment of Span-Loaded Cargo Aircraft Concepts," NASA CR-145034. August 1976.
- [10] Flechner, S.G., Jacobs, P.F., Whitcomb, R.T., "A High Subsonic Speed Wind-Tunnel Investigation of Winglets on a Representative Second-Generation Jet Transport Wing," NASA-TN D-8264, July 1976.
- [11] Ishimitsu, K.K., "Aerodynamic Design and Analysis of Winglets," AIAA Paper No. 76-940, September 1976.
- [12] Gilson, C., "Israel's Aerospace Industry", Flight International, 901 - 912 (April 9, 1977).

- [13] Jane's All The World's Aircraft 1974/75, London.
- [14] Lucchi, C.W., "Calculations of Aerodynamic Coefficients of Aircraft Equipped with Enclosed Propellers", Dornier Report No. 75/46 B, December 1975.
- [15] Kleiner, H., Zimmer, H., "Airfoil Drag Reduction, Part 1: Water Tunnel Studies," Dornier Report No. 74/4 B, April 1974
- [16] Zimmer, H., "Airfoil Drag Reduction, Part 2: Theory of Induced Drag taking into Account Three-dimensionally Deformed Vortex Layers and Application to the Airfoil Design," Dornier Report No. 75/15 B, August 1975.
- [17] Riley, D.R., "Wind-Tunnel Investigation and Analysis of the Effects of Endplates on the Aerodynamic Characteristics of an Unswept Wing," NASA TN 2440, August 1951.
- [18] "New Gulfstream Uses Advanced Design," Aviation Week & Space Technology (November 15, 1976).
- [19] Kelly, T.C., "Some Methods for Reducing Wing Drag and Wing-Facelle Interference," NASA-CR-145627, July 1975.
- [20] Klass, P.J., "Wake Vortex Sensing Efforts Advance," Aviation Week & Space Technology (April 25, 1977).
- [21] Nagel, A.L., et al., "Future Long-Range Transports-Prospects for Improved Fuel Efficiency," NASA TN X 72659, February 1975.
- [22] Stanewsky, E., Zimmer, H., "Development and Wind-Tunnel Testing of three Supercritical Airfoil Profiles for Commercial Aircraft," ZfW 23. Issue 7/8, 246 - 256 (1975).
- [23] Welte, D., "Profile Design of an Airfoil of Present Technology for General Aviation", DGLR-77-27, Berlin, September 13 - 15, 1977.
- [24] Morisset, J., "Avec ses Winglets, l'Arava-202 gagne 500 km sur son rayon d'action," Air et Cosmos (June 11, 1977).
- [25] Menadovitch, M., "Recherches Sur les Cellules Biplanes Rigides D'Envergure Infinie," Publications Scientifiques et Techniques du Ministere de l'Air, Institut Aerotechnique de St.-Cyr, Paris, 1936.
- [26] Olson, E.C., Experimental Determination of Improved Aerodynamic Characteristics Utilizing Biplane Wing Configurations, M.S. Thesis, Mechanical and Aerospace Engineering Department, Univ. of Missouri - Rolla, Rolla, Missouri, 1974.

- [27] Smith, A.M.O., "Aerocynamics of High-Lift Airfoil Systems," AGARD-CP-102, Lissabon, April 1972.
- [28] Friedrichs, R., Hastreiter, W., "Wind-Tunnel Studies of novel Airfoil End Forms," DFVLR-IB 157-75 A 15, 1976.
- [29] Friedrichs, R., Hastreiter, W., Paoletti, C., "Wind-Tunnel Studies of novel Airfoil End Forms, Second Measurement Series," DFVLR-IB 157-77A07, 1977.
- [30] Schauwecker, L., "Wind-Tunnel Experiments with and without Jet Simulation using the 1:8 Whole Model of the DC 28 D2 with an Airfoil of Present Technology," Dornier Experimental Report No. BF60-0579, 1976.
- [31] Proksch, H.J., "New Technology in Future Transport Aircraft - Possibilities for Improving the Airbus Wing in Relation to Drag," Dornier File No. BF10-0964/77.